Arsenic sequestration by metallic iron under strongly reducing conditions

Bhawana Sharma and Purnendu Bose*

Environmental Engineering and Management Programme,
Department of Civil Engineering,
Indian Institute of Technology, Kanpur, Kanpur 208 016, India

The objective of this study was to elucidate the mechanism of arsenic sequestration by metallic iron in strongly reducing conditions. Contacting arsenic with metallic iron in anaerobic batch systems showed considerable reduction in dissolved arsenic concentration. Scanning electron micrographs of the metallic iron surface after contact with arsenic showed evidence of surface depositions. X-ray diffraction patterns of such surfaces showed evidence for the presence of iron arsenide (FeAs and $FeAs_2$) phases, and arsenopyrite (FeAsS) and oripment (As_2S_3) phases respectively, in the absence and presence of dissolved sulphate. Theoretical chemical speciation studies supported the above experimental results. It was thus concluded that strong reducing conditions produced in the vicinity of the anaerobically corroding metallic iron surface result in arsenic sequestration.

Keywords: Arsenic, arsenopyrite, metallic iron, X-ray diffraction.

SEVERAL recent investigations[1–3] have shown metallic iron to be an efficient adsorbent for both arsenic (III) and arsenic (V) under aerobic conditions. The mechanism of sequestration in such cases appears to be the adsorption of arsenic (III) and arsenic (V) on iron oxide minerals, i.e. rust formed on the metallic iron surface as a result of metallic iron corrosion reaction in aerobic conditions[4], according to eqs (1) and (2):

Aerobic iron corrosion:

$$2Fe(0) + O_2 + 2H_2O \rightarrow 2Fe^{2+} + 4OH^-, \quad (1)$$

$$4Fe^{2+} + O_2 + 10H_2O \rightarrow 4Fe(OH)_3(s) + 8H^+. \quad (2)$$

Goldberg and Johnston[5], based on macroscopic measurements, vibrational spectroscopy and surface complexation modelling, reported that arsenic (V) forms inner-sphere complexes with amorphous ferric oxide surface, while arsenic (III) forms both inner- and outer-sphere complexes.

In highly reduced environments and in the presence of iron, arsenic is present as iron–arsenide minerals, e.g. westerveldite[6] and in presence of sulphur arsenic is predominantly sequestered in association with sulphides[7]. The common arsenic-bearing sulphidic minerals that are cited as natural sources of arsenic are arsenopyrite (FeAsS), realgar (AsS), enargite ($CuAsS_4$)[8] and oripment (As_2S_3)[9], with arsenopyrite being the most common[10]. Through experiments carried out in anaerobic conditions, Su and Puls[3] presented strong evidence for reduction of arsenic (V) near metallic iron surface. Ramaswami *et al.*[11] reported arsenic sequestration by metallic iron under anaerobic conditions, and in the presence of sulphate. It was hypothesized that during metallic iron corrosion under anaerobic conditions (eq. (3)), conditions near the vicinity of the iron surface may be sufficiently reducing for the formation of iron–arsenide and iron–arsenic–sulphide phases on the surface of anaerobically corroding metallic iron.

Anaerobic iron corrosion:

$$Fe(0) + 2H^+ \rightarrow H_2 + Fe^{2+}. \quad (3)$$

The objective of the present study was to present evidence in support of the above mechanism.

Iron filings used for arsenic sequestration contained 94.54% iron, 2.34% carbon, 0.031% copper and 0.349% manganese by weight. Surface area of the iron filings was determined to be 0.586 $m^2 g^{-1}$ (BET surface analyzer, Coulter SA 3100, USA). Before use, iron filings were pre-treated for elimination of any oxide coating that may have formed due to prior exposure to the atmosphere.

To determine the extent of arsenic incorporation on the metallic iron surface, 0.75 g of iron filings was taken in 300 ml bottles, which were then filled to the brim with de-aerated de-ionized water, such that no headspace existed. These bottles were maintained for 48 h to ensure initiation of anaerobic iron corrosion. De-aerated stock solution of arsenic (III) was added to the bottles with a syringe, such that arsenic concentration in the bottles was 1000 µg/l. In some bottles, de-aerated sulphate stock solution was added in addition to arsenic (III), such that the sulphate concentration was 250 mg/l in these bottles. The sealed bottles

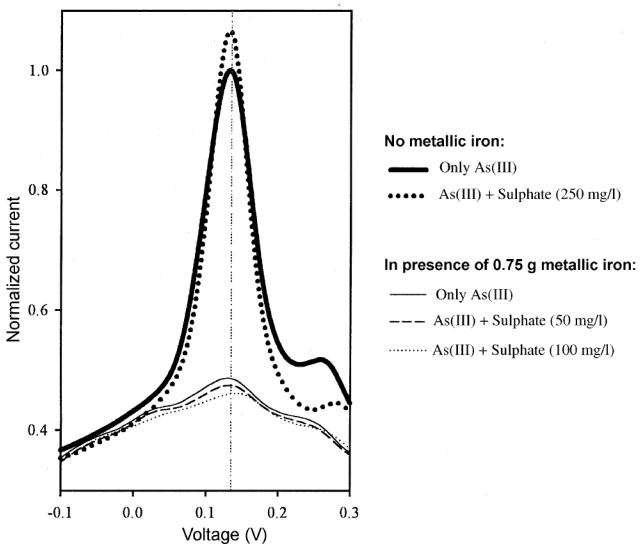

Figure 1. Voltammograms indicating concentration of dissolved arsenic (III) during batch experiments (added arsenic (III): 1000 µg/l).

*For correspondence. (e-mail: pbose@iitk.ac.in)

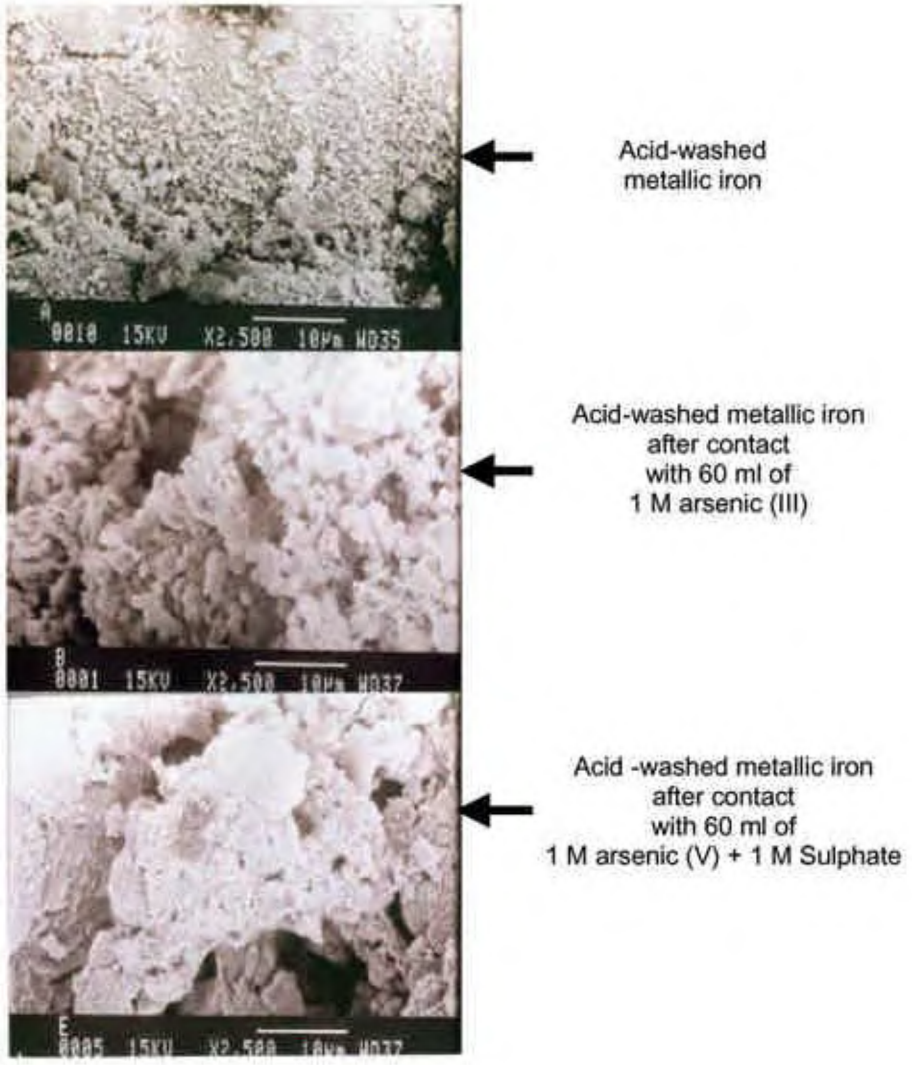

Figure 2. Scanning electron micrographs of acid-washed iron surface before and after arsenic incorporation.

were maintained in agitated condition (end-over shaker) for 4 h. Aqueous samples taken from the bottles were analysed for dissolved arsenic (III) content by anodic stripping differential pulse voltammetry (ASDPV). Suitable blanks, i.e. bottles with no metallic iron, but added arsenic and sulphate were simultaneously analysed. Initial sample pH, measured just after arsenic addition, was 7.5–7.7 during such experiments. These experiments were carried out at room temperature, which was 25 ± 3°C during the experimental duration.

In experiments designed for determination of change in surface properties of metallic iron due to arsenic incorporation, 0.6 g of iron filings was taken in 60 ml plastic bottles, which were then filled to the brim with de-aerated deionized water, such that no headspace existed. The bottles were maintained in this condition for 48 h to ensure initiation of anaerobic iron corrosion. Water was extracted from the bottle with a syringe and replaced with equal volume of de-aerated stock solution containing 1 M arsenic (III) or arsenic (V). Sulphate (1 M) was also added to some bottles. Initial solution pH, measured just after arsenic addition, was 7.5–7.7. All bottles were maintained in agitated condition (end-over shaker) for 48 h. These experiments were carried out at room temperature, which was 25 ± 3°C during the experimental duration. The samples were then centrifuged at 10,000 rpm (REMI C 24, Remi, India) for 15 min to separate the solid phase. The solid sample was dried in nitrogen atmosphere and stored in vacuum desiccators, and subsequently analysed by X-ray diffractometry (XRD) for determination of phase composition and by scanning electron microscopy (SEM) for microstructural analysis.

Dissolved arsenic (III) concentration in aqueous samples was measured by ASDPV (VA Trace 757, Metrohm, Switzerland). Scanning electron micrographs of iron filing samples were obtained using a SEM (Model JXA 840, JEOL, Japan). XRD analyses were performed using X-ray powder diffractometer (Model ISO-Debyeflex

2002, Rich Seifert & Co, Germany) using Cu-K_α radiation (with $\lambda = 1.541841$ Å). The scan rate used was 5 deg/min. The diffraction patterns were analysed using DIFFRAC^{plus} (Release 2001 Eva version 7.0) software (Bruker Advanced X-Ray Solutions) with the aid of JCPDF database available with the software DIFFRAC^{plus} (Release 2001 PDF Maint version 7.0, Bruker Advanced X-Ray Solutions). Analysis was typically done at three points on a particular surface, to ensure that the results were representative of the whole surface.

Results of experiments designed to determine the extent of arsenic incorporation on metallic iron surface are presented in Figure 1. Comparison of normalized voltammograms corresponding to samples without and with addition of metallic iron indicates that considerable decline in the height of voltammograms occurs in the latter cases, suggesting arsenic incorporation on metallic iron in strongly reducing conditions.

Metallic iron samples obtained after arsenic incorporation were examined by SEM for microstructural analysis. Scanning electron micrographs obtained for some metallic iron samples are presented in Figure 2 at 2500 times magnification. The top micrograph in Figure 2 shows the image of the iron surface after acid-washing, but before arsenic incorporation. The iron surface seems to be rough, probably due to pitting corrosion of metallic iron surface caused by chloride ions during acid-washing[12], and largely devoid of any deposits. The middle and lower micrographs in Figure 2 show the images of the metallic iron surface after contact with dissolved arsenic (III) and dissolved arsenic (V) and sulphate respectively, under anaerobic conditions. Clear evidence of surface deposition is seen in both cases. Scanning electron micrographs of other samples taken after arsenic incorporation also showed similar results.

Samples analysed by SEM were also analysed using XRD. Comparative XRD patterns of samples A, B and C, i.e. only iron, iron with arsenic (III), and iron with arsenic (V) respectively, are presented in Figure 3. The XRD pattern of sample A (Figure 3) showed the matching peaks with iron (Fe) (JCPDF 1-1267). The probable phases identified in sample B were iron (Fe) (JCPDF 1-1267), iron arsenide (orthorhombic, $FeAs_2$) (JCPDF 79-251), and iron arsenide (orthorhombic, FeAs) (JCPDF 76-458). The phases identified in sample C (Figure 3) were the same as those in sample B. This suggests that the arsenic incorporation mechanism on the metallic iron surface is similar in samples B and C, and involves arsenic reduction near the iron surface, followed by the deposition of reduced arsenic-bearing phases on the iron surface. No peaks corresponding to iron oxides were noticed in any case, suggesting little or no rust formation under the prevalent anaerobic conditions. Comparative XRD patterns of samples A, D and E, i.e. only iron, iron with arsenic (III) and sulphate, and iron with arsenic (V) and sulfate respectively, are presented in Figure 4. The probable phases identified in sample D were iron (Fe) (JCPDF 1-1267), arsenopyrite/arsenic iron sulphide (AsFeS) (JCPDF 2-946) and orpiment (monoclinic, As_2S_3) (JCPDF 19-84). The phases identified in sample E were the same as those in sample D. This suggests that the arsenic incorporation mechanism in both samples D and E was the deposition of arsenopyrite and oripment phases on the metallic iron surface. As earlier, no peaks corresponding to iron oxides were noticed in any of the above cases.

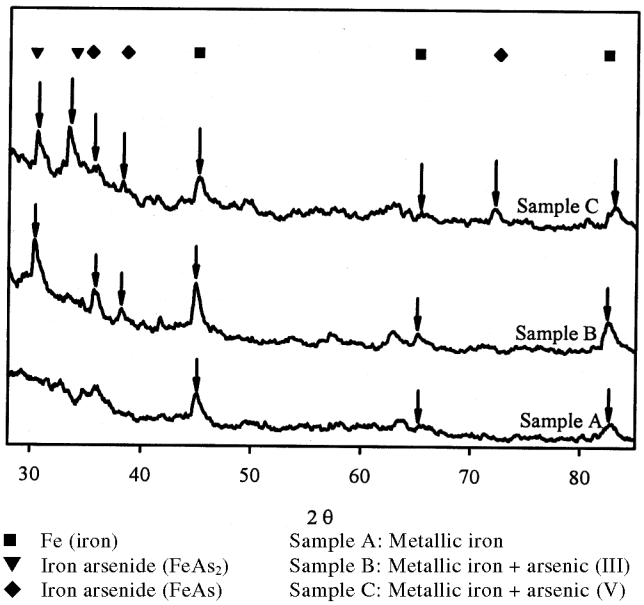

Figure 3. Comparative X-ray diffraction patterns for samples A–C.

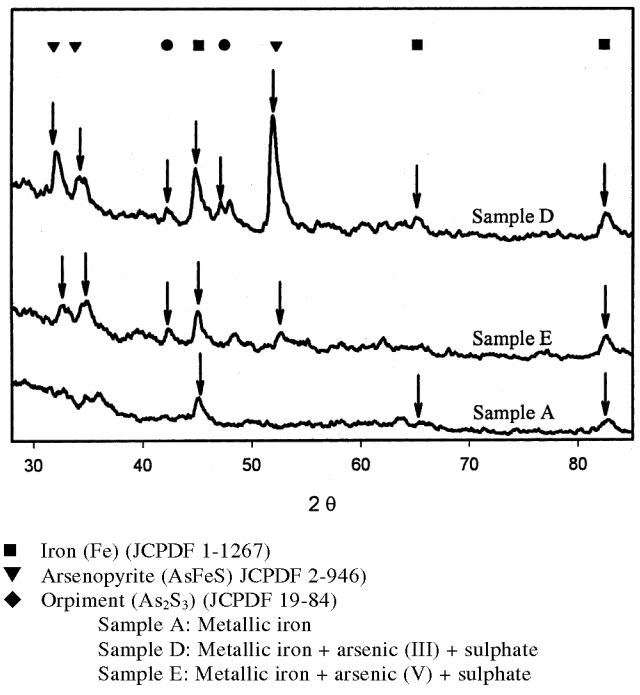

Figure 4. Comparative X-ray diffraction patterns for samples A, D and E.

Theoretical calculations (not reported here) indicate that when metallic iron is contacted with water in anaerobic conditions in the pH range of 7–9, the pE at the metallic iron surface is likely to be between –13 and –9. Theoretical speciation studies with arsenic, iron and sulphur were carried out in the same pH and pE ranges, using MINEQL+, a chemical speciation software. Total species concentrations used were 10^{-6} M for arsenic, and 5×10^{-5} M for iron and sulphur, which are representative of conditions expected near the metallic iron surface. Calculations show that at pE below –11, all arsenic is present in a precipitated form as FeAsS (arsenopyrite) in the pH range of 6 to 10. Speciation calculations in the pH range of 6 to 10 and pE value of –11 (Figure 5 *a*) show that all arsenic is present in the precipitated form, mainly as FeAsS, with transformation of FeAsS to As_2S_3 (oripment) noticeable beyond pH 9.5. Speciation calculation at pE –10 (Figure 5 *b*) also shows that all arsenic is present in precipitated form, however, only As_2S_3 precipitate is observed beyond pH 9.75. Calculations at pE –9 (Figure 6 *a*) indicate FeAsS precipitation up to pH 8.75 and complete solubilization of arsenic at pH greater than 9.75. Calculations at pE –8 (Figure 6 *b*) show no evidence of FeAsS precipitation; however, arsenic is present in precipitated form as As_2S_3 up to pH 9, after which complete solubilization of arsenic is observed. In conclusion, results of Figures 5 and 6 taken in totality provide theoretical support for experimental results presented in Figure 4, i.e. arsenic precipitation as either FeAsS or As_2S_3 is expected on anaerobically corroding metallic iron surface in systems containing sulphate.

The main objective of this study was to elucidate the mechanism for arsenic sequestration by metallic iron under anaerobic conditions. The results presented indicate that:

- Contacting arsenic with metallic iron in anaerobic conditions, both in the presence and absence of sulphate resulted in considerable reduction in dissolved arsenic concentration, which suggested arsenic sequestration by the metallic iron surface.
- SEM of the metallic iron surface after contact with arsenic in anaerobic systems showed evidence of surface depositions.
- XRD patterns of surfaces both before and after arsenic incorporation showed no evidence of iron oxide phases, thus eliminating arsenic adsorption on iron oxide as the mechanism for arsenic sequestration.

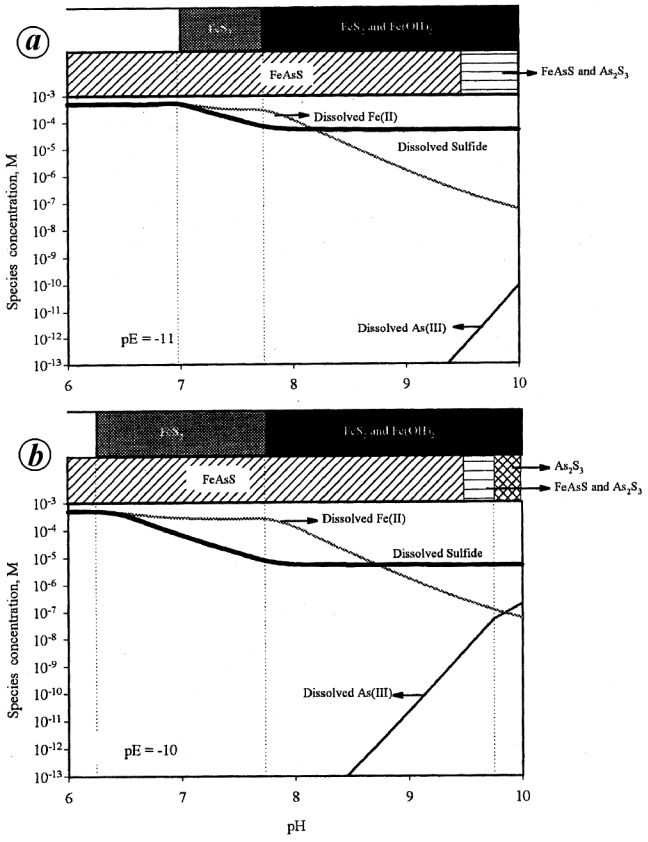

Figure 5. Equilibrium chemical speciation and precipitate formation in a system containing 1 µM arsenic, 500 µM iron and 500 µM sulphur at (*a*) pE = –11 and (*b*) pE = –10; temperature, 25°C.

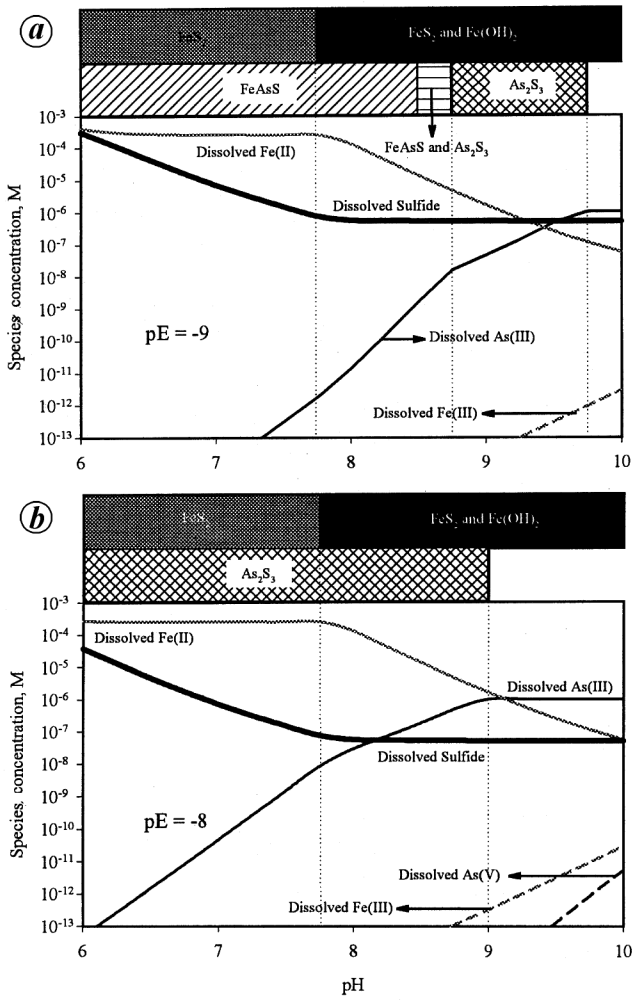

Figure 6. Equilibrium chemical speciation and precipitate formation in a system containing 1 µM arsenic, 500 µM iron and 500 µM sulphur at (*a*) pE = –9 and (*b*) pE = –8; temperature, 25°C.

- XRD patterns of metallic iron surfaces after arsenic incorporation showed presence of iron arsenide (FeAs and $FeAs_2$) phases when no sulphur was present, and presence of arsenopyrite (FeAsS) and oripment (As_2S_3) when sulphur was present.
- Based on the similarity of XRD patterns irrespective of whether arsenic (III) or arsenic (V) was contacted with the metallic iron surface, it was concluded that arsenic incorporation on the metallic iron surface involved arsenic reduction near the iron surface, followed by deposition of reduced arsenic-bearing phases on the iron surface.
- Theoretical chemical speciation studies of a system containing arsenic, iron and sulphur showed precipitation of arsenic-bearing sulphide phases, i.e. FeAsS (arsenopyrite) and As_2S_3 (oripment) under strongly reducing conditions expected in the vicinity of anaerobically corroding metallic iron surface.

In conclusion, these results indicate that adsorption columns and *in situ* reactive barriers containing metallic iron may potentially be efficient in removing dissolved arsenic from water under strongly reducing conditions.

1. Lackovic, J., Nikolaidis, N. P. and Dobbs, G. M., Inorganic arsenic removal by zero-valent iron. *Environ. Eng. Sci.*, 2000, **17**, 29–39.
2. Farrell, J., Wang, J., O'Day, P. and Conklin, M., Electrochemical and spectroscopic study of arsenate removal from water using zero-valent iron media. *Environ. Sci. Technol.*, 2001, **35**, 2026–2032.
3. Su, C. and Puls, R. W., Arsenate removal by zerovalent iron: kinetics, redox transformation, and implications for in situ ground water remediation. *Environ. Sci. Technol.*, 2001, **35**, 1487–1492.
4. Melitas, N., Wang, J., Conklin, M., O'Day, P. and Farrell, J., Understanding soluble arsenate removal kinetics by zerovalent iron media. *Environ. Sci. Technol.*, 2002, **36**, 2074–2081.
5. Goldberg, S. and Johnston, C. T., Mechanism of arsenic adsorption on amorphous oxides evaluated using macroscopic measurements, vibrational spectroscopy, and surface complexation modeling. *J. Colloid Interface Sci.*, 2001, **234**, 204–216.
6. Utsunomiya, S., Peters, S. C., Blum, J. D. and Ewing, R. C., Nanoscale mineralogy of arsenic in a region of New Hampshire with elevated As-concentrations in the groundwater. *Am. Mineral.*, 2003, **88**, 1844–1852.
7. Loeppert, R. H., Arsenate and arsenite retention and release in oxide and sulfide dominated systems. Technical Report No. 176, Texas Water Resources Institute, College Station, Texas, 1997.
8. Bhowmik, A., Mineralogical study of arsenic contamination of an aquifer system in West Bengal. M.Tech. thesis, Department of Civil Engineering, IIT, Kanpur, 1999.
9. Moore, J. N., Ficklin, W. H. and Johns, C., Partitioning of arsenic and metals in reducing sulfidic sediments. *Environ. Sci. Technol.*, 1988, **22**, 432–437.
10. Battey, M. H., *Mineralogy for Students*, Longman Scientific and Technical, 1990, 2nd edn.
11. Ramaswami, A., Tawachsupa, S. and Isleyen, M., Batch-mixed iron treatment of high arsenic waters. *Water Res.*, 2001, **35**, 4474–4479.
12. Bardwell, J. A., Fraser, J. W., MacDougall, B. and Graham, M. J. Influence of anodic oxide film on pitting of iron. *J. Electrochem. Soc.*, 1992, **139**, 366–370.

Received 5 November 2005; revised accepted 8 March 2006

Determination and quantification of camptothecin in an endophytic fungus by liquid chromatography – positive mode electrospray ionization tandem mass spectrometry

Touseef Amna, Ravi K. Khajuria*, Satish C. Puri, Vijeshwar Verma and Ghulam N. Qazi

Regional Research Laboratory, Canal Road, Jammu 180 001, India

This communication describes the detection of Camptothecin (CPT) in an endophytic fungus and application of gradient reverse phase HPLC method with diode array and MS/MS detection for quantification of the said compound. The extract of fungus *Entrophospora infrequens* isolated from the inner bark of *Nothapodytes foetida* plant was chromatographed on a Merck (250 × 4.6 mm, 5 μm) column, maintained at 30°C, and analysed by positive mode electrospray ionization tandem mass spectrometry on a mass spectrometer in a single reaction monitoring system. The mobile phase consisted of a linear gradient of water, acetonitrile from 10 to 98% in 35 min. The quantity of CPT in the extract was estimated on the basis of linear calibration curves obtained in the concentration range of 5 to 50 ng with standard CPT. Fungus grown under surface culture method accumulated 40 mg CPT/kg dry cell mass, which is far lower than that present in the plant source from where the organism was isolated. This report on the accumulation of CPT in a fungus may be a starting point for improving the productivity of CPT in this isolate.

Keywords: *Enterophospora infrequens*, liquid chromatography, *Nothapodytes foetida*, single reaction monitoring, tandem mass spectrometry.

CAMPTOTHECIN, often abbreviated as CPT (Figure 1), and its analogues are naturally occurring group of quinoline alkaloids depicting profound cytotoxic activity[1]. Various plant species such as *Camptotheca acuminata*, *Ophiorrhiza mungo*, *Ervatomia hyneana* and *Nothapodytes foetida* are known sources of this phytochemical[2]. The supply of CPT depends primarily on the abundant availability of plants such as *C. acuminata*. Many parts of this plant can be used to extract CPTs[3]. The overexploitation of this source rendered the plant as an endangered species all over the globe, especially in China. The gene pool of this plant is very small in countries like USA[4]. Literature survey on camptothecin revealed that the molecule occupies an important position among the plant-based anti-cancer drugs[5–21]. In order to conserve the germplasm, a need was felt to look for alternate sources for this class of natural products. Sustained search in this direction led to the isolation of an

*For correspondence. (e-mail: khajuriark@yahoo.com)